Model-driven Approach to Improve Sago Drying with a Fluidized Bed Dryer

Nur Tantiyani Ali Othman* and Nurfadilah Izaty Senu

Department of Chemical and Process Engineering, Faculty of Engineering and Built Environment, Universiti Kebangsaan Malaysia, 43600, Bangi UKM, Selangor, Malaysia

ABSTRACT

This study presents a model-driven approach to enhance the efficiency of sago drying utilizing a two-dimensional fluidized bed dryer (FBD). ANSYS® DesignModeler™ 2020 R2 software was employed to simulate the drying profile, considering variations in sago bagasse particle diameter (ranging from 500 to 2000 µm), hot air temperature (ranging from 50 to 90°C), and inlet air velocity (ranging from 1.5 to 2.1 m/s). The simulation results provided valuable insights into the interplay between these critical drying parameters. The model enabled the prediction of moisture content profiles during the sago drying process under different conditions, thereby facilitating comprehension of the system's behavior. Using Design Expert® 7.00 (DX7), considering energy efficiency and product quality, an optimal set of conditions for sago drying was determined at 2000 µm, 90°C and 2.1 m/s. This approach not only streamlined the drying process but also significantly reduced energy consumption while ensuring consistent and high-quality sago. The findings of this research offer a practical and sustainable solution for sago producers, which, when applied, can contribute to improved product quality, reduced production costs, and enhanced food security in the region. Furthermore, the model-driven approach and the integration of specialized software tools demonstrate the potential for broader applications in optimizing various drying processes in the food industry.

Keywords: Computational fluid dynamics, drying, fluidized bed dryer, respond surface methodology, sago waste

INTRODUCTION

Sago, a vital source of carbohydrates for many Southeast Asian communities, undergoes a protracted and inefficient drying process, significantly influencing its quality, shelf life, and economic viability. Southeast Asia produces nearly 60 million tons of sago starch annually (Wee et al., 2017). Malaysia is currently the world's largest sago producer, followed by Indonesia and Papua New Guinea, which account for around 94.6% of global sago production (Naim et al., 2016). The development of the agricultural industry has resulted in an increment in agricultural waste, which is largely cellulose-rich waste such as sago bagasse (Rashid et al., 2016). The increase in sago production yearly directly increases the amount of sago bagasse produced. Disposal of sago bagasse in rivers causes river pollution. Therefore, more studies on sago bagasse need to be conducted so that this sago bagasse has economic value and, thus, the environmental pollution that occurs due to the disposal of sago bagasse in the river can be minimized.

The primary purpose of this research is to revolutionize the sago drying process, making it more efficient, sustainable, and economically viable. As a staple food for many communities, sago plays a crucial role in food security, and its production impacts the livelihoods of numerous individuals. The traditional drying methods result in inconsistent product quality and entail significant energy consumption, making the production process economically challenging. This research is motivated by the need to address these pressing issues, enhance the quality of sago products, and make the sago industry more resilient.

Various methods have been carried out to convert sago bagasse into more valuable products, such as animal feed, through drying and fermentation. Sago bagasse needs to be dried before being used as animal feed as it is easily damaged due to its high moisture content. Drying is a highly energy-intensive operation used in industry, with an average of 12% of total energy consumption consumed in manufacturing (Sarker et al., 2015). Normally, an experiment conducted in the laboratory to develop this dryer model requires considerable time and effort and uses high costs (Malekjani & Jafari, 2018). Thus, this study applied the computational fluid dynamics (CFD) method to develop a dryer model, as this method is an effective way of overcoming these problems of high energy consumption. Besides, the CFD method can provide an excellent understanding of the transport phenomenon during the drying process and improve process control, leading to drying optimization and better quality of sago waste.

One of the common dryers, the fluidized bed dryer (FBD), has been widely used in drying final products or raw materials, such as agricultural produce, due to their advantages over other dryers, such as spray dryers and cabinet-type dryers. FBD has good mixing efficiency and a high heat and mass transfer rate between solids and gases (Zhang et al.,

2017). Moreover, FBD has a large contact surface area between solids and gases, produces high thermal inertia of solids, and can reduce drying time without damaging heat-sensitive materials (Rosli et al., 2020).

This innovative research combines FBD technology with traditional food production methods using a multidisciplinary approach. Insights into the complex drying process and the interaction of multiple variables can be obtained by employing ANSYS software for simulation. This innovative approach allows us to optimize the drying parameters to achieve a delicate balance between drying efficiency and preserving the nutritional and sensory qualities of sago. Furthermore, by employing the response surface methodology using Design Expert® 7.00 (DX7) software, the optimal conditions for sago drying can be determined, thereby streamlining the process and minimizing energy consumption.

Numerous researchers have applied the CFD method to dry their products in the FBD. For example, Arumuganathan et al. (2010) dried their mushroom in the FBD at the optimum temperature of 60°C, and Anthony and Shyamkumar (2016) dried sand particles in the FBD using ANSYS© software. Besides, Mortier et al. (2011) applied Eulerian-Eulerian two-fluid CFD models to analyze the behavior of dried wheat grain in the FBD. The study found that higher temperatures and inlet air velocities significantly impact the drying rate. This effect was observed in various industries such as oil palm fronds, millet pearl, coconut, wheat, grain, and sago bagasse industries (Assawarachan, 2013; Azmir et al., 2018; Li-Zhen et al., 2019; Maheswari, 2015; Othman et al., 2021; Puspasari et al., 2014).

Prior research has demonstrated the successful application of the CFD method in observing and analyzing the fluidizing rate within the FBD. This method offers the advantages of efficiency and cost-effectiveness. Thus, this research introduced a model-driven approach to improve sago drying using an FBD, employing ANSYS software to simulate the drying profile. In this study, various key drying parameters such as particle diameter of sago bagasse (ranging from 500 to 2000 μm), hot air temperature (varying from 50 to 90°C), and inlet air velocity (spanning from 1.5 to 2.1 m/s) were systematically utilized to optimize sago drying. The potential outcomes of this research hold promise for sago producers, the communities that rely on sago as a food source, and the broader food industry. The findings could reduce production costs, minimize post-harvest losses, and improve food security. Furthermore, utilizing the model-driven approach and specialized software tools provides opportunities for enhancing efficiency in different drying processes within the food industry, underscoring the potential for innovative and environmentally friendly solutions in food processing. This research aims to reconcile the disparity between traditional methods and technological advancements, promoting a more promising and environmentally friendly future for sago production.

METHODS

Development of Geometry and Mesh

In the drying process, a slurry of sago waste was dried using the FBD machine. Model Retsch TG 200 has a diameter of 220 mm and a height of 520 mm, including the filter bag, as shown in Figure 1(a), and Figure 1(b) shows the top view of a sample of particle sago that dried in the FBD. For this study, a 2D model of FBD is developed and designed using ANSYS® DesignModeler™ 2020 R2 software based on studies by Othman et al. (2021), as shown in Figure 2. Several assumptions were made, and equations were formulated to solve the simulation problem. Subsequently, the investigation ascertained the most favorable drying conditions by utilizing the response surface method (RSM).

The ANSYS® DesignModeler™ 2020 R2 software was used to develop a 2D model of an FBD based on the TG 200 FBD model. The height of the FBD model is 220 mm by 180 mm wide. The initial height of the sago waste bed in the dryer is 22.83 mm. Then, mesh development on the FBD model is accomplished using ANSYS© Meshing. The mesh size varies from 1-4 mm, with the shape of the resulting mesh being a hexahedral shape. A mesh dependency test was performed to obtain the most suitable mesh size. Figure 3 shows the 2D FBD model with 4 mm mesh.
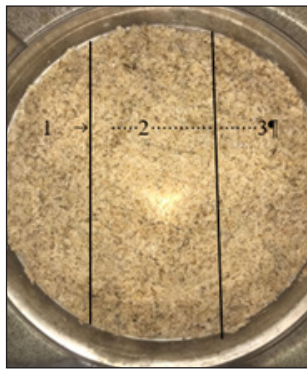

(a)	(b)

Figure 1. (a) A model Retsch TG of FBD; and (b) a sample of dried sago from the top view
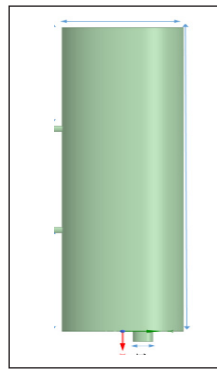
*Figure 2.* Two-dimensional model of the FBD
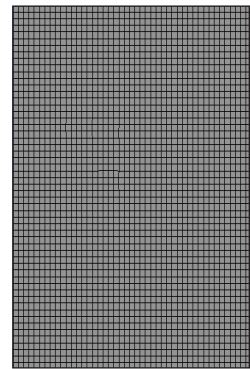
Figure 3. Schematic diagram of the 2D FBD model with 4 mm mesh

CFD Modelling

The CFD simulations have made some assumptions, assuming that no chemical reactions occur during the drying period. The gases and solids exhibit good miscibility. However, the slip condition was not established. The initial moisture content of sago waste was 40% based on its wet weight, while the final moisture content after the drying process was 10% based on its dried weight. In this study, the Eulerian-Eulerian model approach was used to

analyze the hydrodynamic and heat transfer properties in the FBD. The turbulence model was applied as there was a turbulent flow in the dryer, and the realized k-ε model was used due to minimal computational requirements. The transport and heat models were also utilized to account for the heat transfer between gases and solids. The air in this model represented the primary phase, the sago waste represented the secondary phase, and water vapor represented the tertiary phase. The SIMPLE algorithm was employed to achieve convergence. Table 1 details the settings set on the ANSYS© Fluent simulation code.

In the ANSYS© Fluent simulation, the creeping flow and turbulent modules were used to simulate fluid flow at very low Reynolds numbers where the inertia term in the Navier-Stokes equation can be ignored. The governing Equations 1 to 4 solved the fluid flow problem. Furthermore, the fluid mechanics in the FBD is a conservation of mass, momentum, and energy where $\vec{v}_q$ is a velocity for q phase, p is pressure, $\dot{m}_{pq}$ is a mass transfer from p phase to q phase, $\dot{m}_{qp}$ is a mass transfer from q phase to p phase, h is a heat transfer coefficient, ρ is a density, q is a heat flux, ε is a volume fraction, Q is a heat

Table 1
ANSYS© Fluent setting

Input settings		Variables/ Parameters in ANSYS©	
General	Solver	Type	Pressure-based
		Velocity	Absolute
	Time	Transient	
Model	Multiphase (Eulerian)	Primary phase	Air
		Secondary phase	Sago waste
		Tertiary phase	Water vapor
		Particle size	2000 μm
		Phase interaction	Mass transfer Evaporation-condensation
	Viscous	k-epsilon	Realizable
		Near-wall treatment	Scalable wall functions
		Turbulence Multiphase model	Dispersed
	Species	Species transport	H_2O vapor
Materials	Fluid	N_2, O_2, sago, H_2O (liquid), H_2O (vapor)	
	Mixture	Sago bagasse - sago, H_2O (liquid)	
Boundary conditions	Inlet (Air)	Momentum	Velocity magnitude (m/s) -2.1 Turbulence intensity- 5%
		Thermal	Temperature (˚C) - 90
Solution	Methods	Scheme	Phase coupled SIMPLE
Initialization	Hybrid Initialization	Species settings	Sago bagasse H_2O (l) – 0.4
Calculation	Step time	35	
	Time step size	0.001 s	

transfer rate, v is a vector velocity, H is a latent heat and τ is a shear stress tensor (Othman et al., 2021).

Conservation of mass

$$\frac{\delta}{\delta t}\left(\alpha_q \rho_g\right) + \nabla.\left(\alpha_q \rho_q \overrightarrow{v_q}\right) = \sum_{p=0}^{n}\left(\dot{m}_{pq} - \dot{m}_{qp}\right) + S_q \qquad [1]$$

Conservation of momentum

$$\frac{\delta}{\delta t}\left(\varepsilon_s \rho_s\right) + \nabla.\left(\varepsilon_s \rho_s v_s\right) = 0 \qquad [2]$$

Conservation of energy
(i) For the gas phase

$$\frac{\delta}{\delta t}\left(\varepsilon_g \rho_g h_g\right) + \nabla.\left(\varepsilon_g \rho_g v_g h_g\right) = -\varepsilon_g \frac{\delta p_g}{\delta t} + \overline{\overline{\tau_g}}:\nabla\overrightarrow{v_g} - \nabla\vec{q}_g + Q_{sg} + \dot{m}\Delta H_{vap} \qquad [3]$$

(ii) For solid phase

$$\frac{\delta}{\delta t}\left(\varepsilon_s \rho_s h_s\right) + \nabla.\left(\varepsilon_s \rho_s u_s h_g\right) = -\varepsilon_s \frac{\delta p_s}{\delta t} + \overline{\overline{\tau_s}}:\nabla\vec{u}_s - \nabla \vec{q}_s + Q_{gs} - \dot{m}\Delta H_{vap} \qquad [4]$$

Analysis of Moisture Content

The moisture content analysis of sago waste at different variables was carried out once the 2D FBD model was successfully designed. A validated model was used to study the drying times for all variable conditions to achieve the desired final moisture content of 10% based on the average volume fraction of sago waste in FBD. At the beginning of the simulation, the volume fraction of sago waste in the FBD was set as 0.60. The simulation was carried out until the average value of the volume fraction of sago waste reached 0.42, equivalent to 10% moisture content.

Then, the effect of temperature on the moisture content of sago waste in FBD was studied. At the beginning of the simulation, the boundary conditions were changed to the temperature values of T=50, 60, 70, 80, and 90°C, while the particle diameter and inlet air velocity were constant in dp=2000 μm and v_i=2.1 m/s. Next, the effect of inlet air velocity on the moisture content of sago waste was studied at v_i=1.5, 1.65, 1.8, 1.95, and 2.1 m/s while the sago diameter and air temperature were constant in dp=2000 μm and T=90°C. At the beginning of the simulation, the velocity of the sago waste was set at 0 m/s to indicate that the bed remained at the initial position. Then, different size diameters of sago, dp=500, 1250, and 2000 μm, were used to study their effects on drying. The boundary conditions were set at an air temperature of T=90°C and an inlet air velocity of v_i=2.1 m/s. Based on these manipulated parameter conditions, the fractional contour of the volume of sago waste in the FBD was observed occasionally.

Mathematical Modelling of Drying Curves

The RSM method, a Design Expert® 7.00 (DX7) software, was used to optimize the sago drying process and parameter. The mixed design used was D-Optima, and the independent variables were the temperature, diameter of sago waste, and velocity of inlet air. The temperature was set up between 50 to 90°C, the range of particle diameter of sago waste was set to 500 to 2000 μm, and the inlet air velocity was between 1.5 to 2.1 m/s. Three code levels for each variable were defined as -1, 0, and +1, representing low, intermediate, and high levels, respectively. The details of the independent variables and levels used in the study are shown in Table 2, while Table 3 shows the central composite design and reaction results.

Table 2
Independent variables and levels used in the study

Independent variables	Unit	Symbol	Level		
			Low (-1)	Medium (0)	High (+1)
Temperature	°C	A	50	70	90
Inlet air velocity (m/s)	m/s	B	1.5	1.8	2.1
Sago bagasse diameter	μm	C	500	1500	2000

Table 3
Central composite design and response results

Run	Factor 1 A: Temperature (°C)	Factor 2 B: Air velocity (m/s)	Factor 3 C: Sago bagasse diameter (μm)	Response 1 Moisture content (%)	Response 2 Deff x 10^{-2} (m²/s)
1	50	1.5	500	25.02353	1.161982
2	90	1.5	500	20.84443	1.248123
3	50	2.1	500	13.22698	1.235517
4	90	2.1	500	10.33	1.259678
5	50	1.5	2000	22.4063	1.217133
6	90	1.5	2000	20.00562	1.304325
7	50	2.1	2000	14.7994	1.223436
8	90	2.1	2000	10.72495	1.305112
9	50	1.8	1250	19.75632	1.254163
10	90	1.8	1250	15.26491	1.303011
11	70	1.5	1250	22.09479	1.29986
12	70	2.1	1250	12.11061	1.299335
13	70	1.8	500	16.78013	1.225012
14	70	1.8	2000	19.63581	1.308527
15	70	1.8	1250	16.41505	1.299335
16	70	1.8	1250	16.41505	1.299335
17	70	1.8	1250	16.41505	1.299335
18	70	1.8	1250	16.41505	1.299335
19	70	1.8	1250	16.41505	1.299335
20	70	1.8	1250	16.41505	1.299335

Response Surface Analysis

The RSM is a statistical method that depends on variables, and each dependent parameter depends on a different input variable (control factor). Each variable has a mathematical relationship with the experimental parameter by a nonlinear polynomial equation with square terms, the interaction of two-factor terms, linear terms, and fixed terms as expressed in Equation 5 (Majdi et al., 2019), where "Res" indicates a reaction (moisture content and moisture diffusivity (D_{eff}), A, B, and C are codes for the values of temperature, inlet air velocity, and diameter of sago waste. The quality of the polynomial model is expressed using the coefficients of determination R^2 and R^2-adjusted. Statistical significance was validated using accuracy factors and F tests.

$$Res = \alpha_0 + \alpha_1 A + \alpha_2 B + \alpha_3 C + \alpha_{11} A^2 + \alpha_{22} B^2 + \alpha_{33} C^2 + \alpha_{12} AB + \alpha_{13} AC$$
$$+ \alpha_{23} BC \qquad [5]$$

RESULTS AND DISCUSSION

The study began with a meshing dependency test for the FBD model, followed by model validation by comparing the simulation results with the previous experimental study by Rosli et al. (2020). The 1.5 mm mesh size was selected as the suitable mesh to be used throughout this simulation due to its constant and stability of the test results. Once the 2D FBD model was developed, the final moisture content of the dried sago was determined at various conditions: temperature (50–90°C), inlet air velocity (1.5–2.1 m/s), and sago particle diameter (500–2000 μm). In summary, the simulation results demonstrated that increasing the air velocity and temperature at the inlet led to a higher drying rate. In addition, the diameter of sago waste solely influenced its moisture content when subjected to low drying temperatures. Subsequently, the RSM analysis was also carried out, and the optimum parameter values for drying sago were determined as dp=2000 μm, T=90°C, and v_i=2.1 m. /s.

Effect of Temperature on Moisture Content

Figure 4 shows the fractional contours of the sago volume fraction in the FBD during drying time of 0–0.017 s at different temperature ranges: T=50–90°C. Under fast step conditions, the simulation was conducted to observe contour patterns at five specific drying times (t=0, 5, 10, 15, and 17 s) to determine the moisture content of sago waste in the FBD. The color bar represents the volume fraction of sago in the final sago waste after the drying process, where the red color indicates the highest sago fraction in the final sago waste with a value of 0.6, and the blue color indicates the lowest sago volume fraction.

The simulation results in Figure 4 show that at the beginning of the drying process, the partial area of the FBD is covered by the maximum fraction of sago waste, which is shown
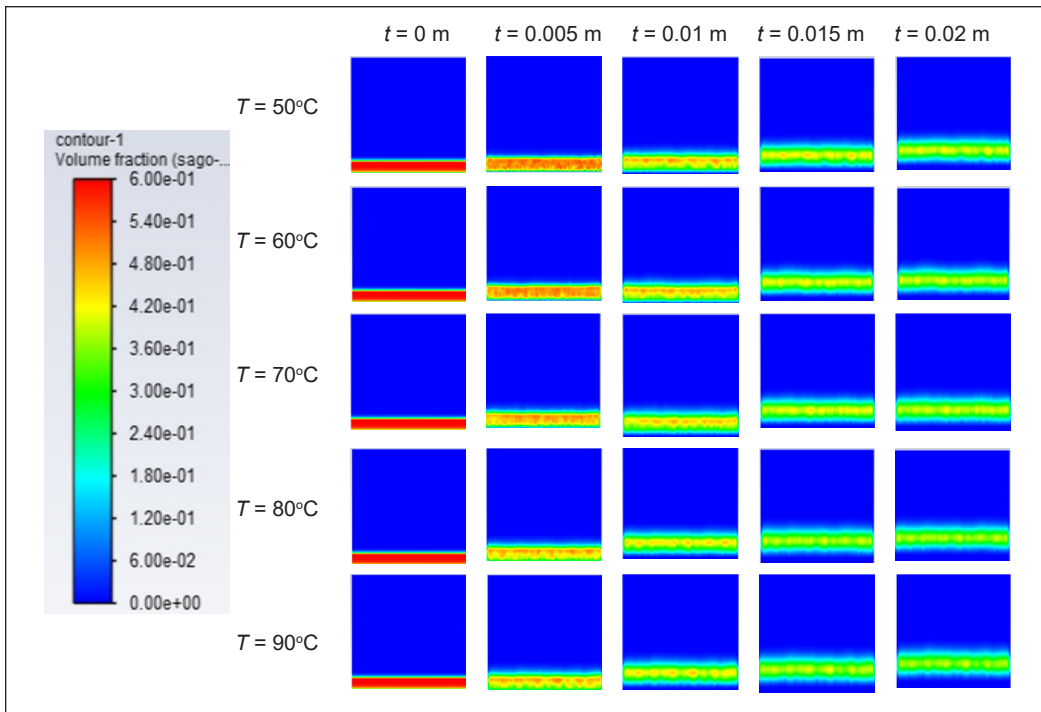
Figure 4. The contour of sago waste volume fraction at various temperatures: 50–90°C

by the red color at the bottom of the FBD area, because the sago waste is assumed to be already in the FBD with the height of the sago bed being 0.02283 m. The initial volume fraction of sago waste in the FBD is 0.6. However, as the evaporation process reduces the water content in the sago waste, the volume fraction of sago waste gradually decreases during the drying process. Furthermore, it indicates that the proportion of sago in the FBD is consistently diminishing. The FBD demonstrates the presence of fluidized sago waste, along with a hot air supply that enhances particle mobility and decreases the moisture content of the sago waste (Tamboli et al., 2018). Meanwhile, at the end of the drying process, t=0.017s, the yellowish-green color contour shows that the volume of sago waste in the FBD is 0.45 and 0.42. It shows that the moisture content of sago waste has been reduced from 40% to around 10-15% after going through the drying process in this FBD model.

Based on Figure 4, the drying of sago waste at T =90°C shows the smallest yellow spots on the volume contour of sago waste at the end of drying; t= 0.017 s. It indicates that the moisture content of sago waste is relatively lower at 90°C than at other drying temperatures. The moisture content values of sago waste obtained at the end of drying for the temperatures of T=50°C, 60°C, 70°C, 80°C and 90°C are MCf=14.8%, 14.3%, 13.1%, 11% and 10.7%, respectively, indicating that the final moisture content of sago waste is relatively higher at lower drying air temperatures. In addition, to achieve the final moisture content of 10%, the drying time should be increased for the drying temperatures

of T=50°C, 60°C, 70°C, and 80°C. It can be concluded that a high drying temperature is required to dry the sago waste quickly. Thus, a drying temperature of T=90°C is optimal for quickly drying the sago waste. In addition, a study has also proven that when the incoming air temperature increases, the drying time can be reduced (Antony & Shyamkumar, 2016). Thus, a drying temperature of T=90°C is the best and optimum temperature to dry sago.

Figure 5 shows the effect of temperature on the final moisture content of sago waste and drying time at different inlet air velocities. The initial moisture content of sago waste before the drying simulation process is 40%. It is shown that as the drying temperature increases, the percentage of
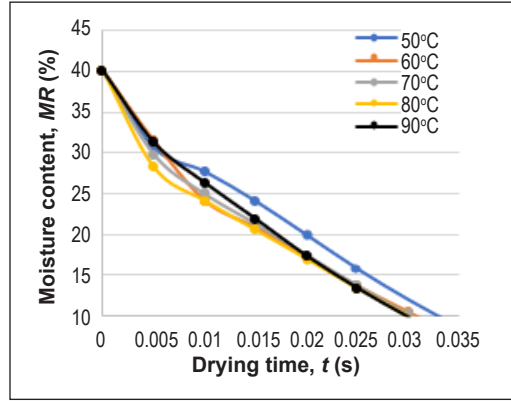

(a)
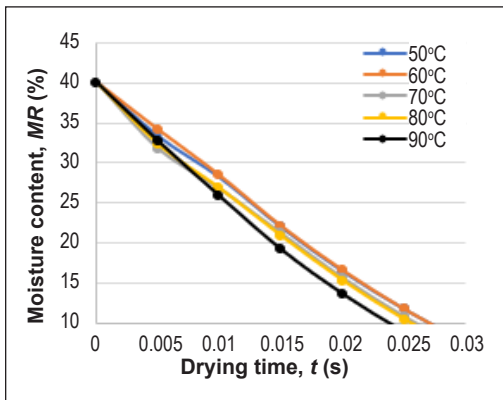
(b)
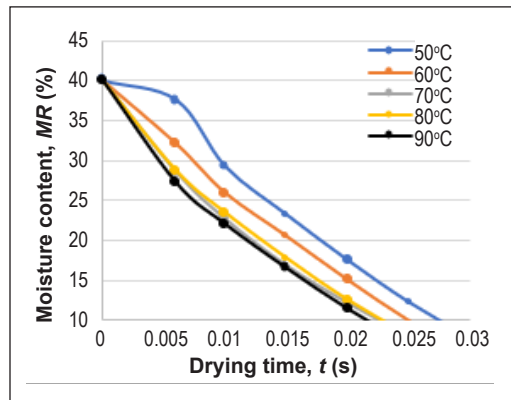
(c)
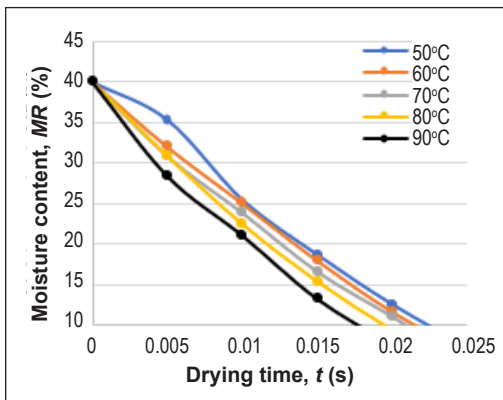
(d)
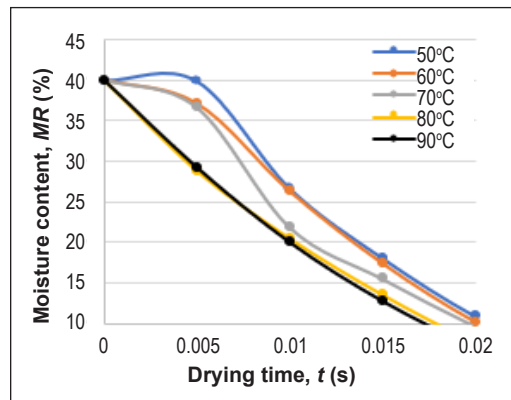
(e)

Figure 5. Moisture content against drying time at a diameter of 2000 μm with different temperatures and air velocities: (a) v_i=1.50 m/s; (b) v_i=1.65 m/s; (c) v_i=1.80 m/s; (d) v_i=1.95 m/s; and (e) v_i=2.10 m/s

final moisture content of sago waste decreases. In addition, as the drying time increases, the final moisture content of sago waste also decreases. The moisture content percentage of sago waste decreases rapidly at high and low temperatures. At T=50°C, the percentage decrease in moisture content of sago waste is relatively slow. Figure 5(e) shows that at T=90°C, a moisture content of 10% is reached within t=0.017s, while at T=50°C, it takes a longer drying time of t=0.021s to achieve a final moisture content of 10%. At a drying temperature of T=80°C, the moisture content of sago waste reaches 10% within t=0.018s, followed by T=70°C and T=60°C with the drying time between t=0.019s and t=0.020s, respectively. The simulation results show that the higher the drying temperature, the faster the moisture content of sago waste reaches 10% because the incoming air temperature is inversely proportional to the drying time and because the air temperature affects the permeation of moisture during the drying process (Gazor & Mohsenimanesh, 2010). At higher temperatures, the particles absorb more heat for water evaporation than at lower temperatures; thus, the evaporation rate increases (Luthra & Sadaka, 2020). The studies by Nasir et al. (2021) have also proven that sago waste dries faster at high temperatures than at low drying temperatures.

Effect of Air Velocity on Moisture Content

Simulations were performed repeatedly by manipulating five inlet air velocities at v_i=1.50, 1.65, 1.80, 1.95 and 2.10 m/s, while the temperature is kept constant at T=90°C with dp=2000 μm based on the minimum and maximum experiments data conducted by Rosli et al. (2020). Figure 6 shows the contours of the volume fraction of sago waste in the FBD at different inlet air velocities within the drying times of t=0.017 s. The contour patterns of the sago volume fraction are observed at 0 s, 0.005 s, 0.10 s, 0.015 s, and 0.017 s. At the beginning of the simulation, t=0 s, the sago waste bed is maintained at a fixed position of 0.02283 m. As the drying process takes place within t=0.005 s, fluidization begins to occur, and the sago bed begins to act as a fluid when the incoming air interacts with the particle layer. This incoming air produces an attraction to overcome the force of gravity (Han, 2015). During this initial period, a rapid increase in bed height is observed until the bed reaches its maximum height. It occurs due to fluidization onset, which is called the fluidization minimum (Dechsiri, 2004). The particle concentration at the bottom area tends to rise uniformly. It indicates a uniform gas entry velocity according to the fluidized characteristics of the FBD (Shukrie et al., 2016).

At the end of the drying process at t= 0.017 s, the yellowish-green color contour shows that the volume of sago waste in the FBD is between 0.42=0.48. It shows that the moisture content of sago waste has been reduced from 40% to 10-20% after going through the drying process in this FBD model. The color contour bars show the fewest patches of yellow at v_i=2.10 m/s air velocity, followed by v_i=1.95, 1.80, 1.65, and 1.50 m/s. The FBD exhibits
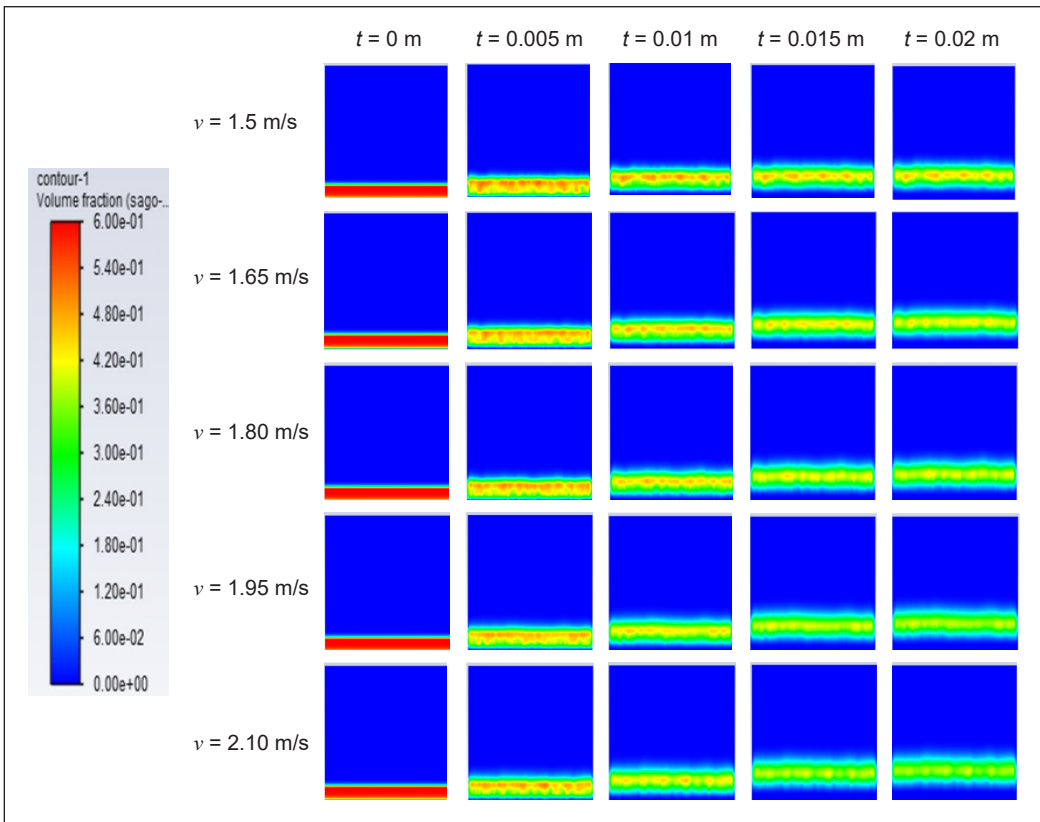
Figure 6. Contour of sago waste volume fraction at air velocity, v_i=1.5-2.1 m/s

a state of fluidized sago, facilitated by the introduction of hot air, effectively decreasing sago waste's moisture level (Rosli et al., 2018). The velocity of the inlet air affects the sago waste's drying process. At higher inlet air velocities, the volume of sago waste in the FBD decreases rapidly. It is supported by a study by Norhaida et al. (2020), which found that increased velocities led to reduced drying times.

Figure 7 shows the effect of inlet air velocity on the final moisture content of sago waste and drying time at different temperatures. It shows that the drying rate initially increases with the drying time before it decreases until the sago has dried to the desired final moisture content because free water is easier to evaporate at the beginning of drying and bound water that is difficult to rise to the surface of the material, so the rate of water evaporation decreases (Hasibuan et al., 2018). However, when the air velocity is increased, the drying rate increases, where the highest drying rate is at the inlet air velocity of v_i=2.1 m/s, which has the shortest drying time. It indicates that the drying rate is higher at higher air velocities due to higher heat and mass transfer between fluidized air and sago waste as air velocity increases (Halim et al., 2020). Also, this is evidenced by a previous where the highest drying rate occurred at a velocity of v_i=2.1 m/s, which resulted in the shortest drying time (Rosli et al., 2020).
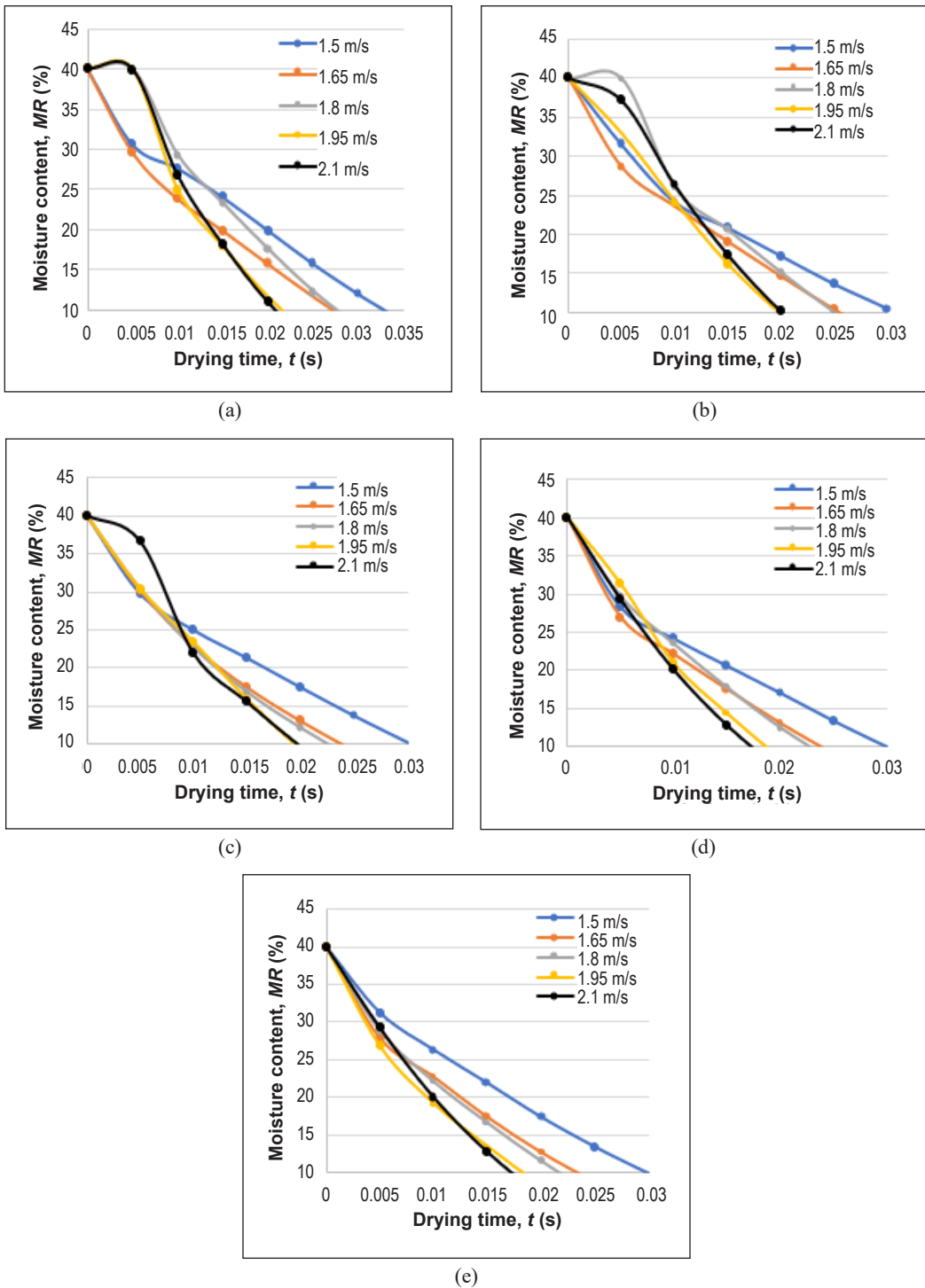
Figure 7. Moisture content against drying time at the diameter of 2000 μm with different air velocity temperatures and temperatures: (a) T=50°C; (b) T=60°C; (c) T=70°C; (d) T=80°C; and (e) T=90°C

Effect of Diameter of Sago Bagasse on Moisture Content

Various ranges of particle diameters of sago waste d_p=500, 1250, and 2000 μm were studied to determine its effect on the final moisture content of 10%. Figure 8 shows the moisture content of sago waste against drying time at different sago waste diameters of d_p=500, 1250, and 2000 m at T=50°C and v_i=2.1 m/s. It shows that the moisture content directly decreases with increasing drying time. Besides, the sago waste diameter of d_p=500 μm reaches a moisture content 10% faster than other sago diameters. At T=50°C, the minimum drying times achieved for sago waste diameter of d_p=500,1250, and 2000 μm are t=0.019, 0.021, and 0.021s, respectively. The smaller particle fractions have a larger surface area, and thus, they can dry faster (Wang & Chen, 2000). In addition, the moisture transport distance within the particles decreases as the particle size decreases, and the time required to dry the particles increases with the particle size increase (Pusat et al., 2015).

For T=70°C, the minimum drying times achieved for sago waste diameter of d_p=500 ,1250, and 2000 μm are t=0.018, 0.019, and 0.020s, respectively. Meanwhile, At T=90°C, the sago waste diameters of d_p=500, 1250, and 2000 μm reach a moisture content of 10.3%, 10.6%, and 10.7% at the time of drying of t=0.017s. The impact of sago particle diameter on the moisture content of sago waste is more pronounced at lower drying temperatures than at higher temperatures. The drying process is primarily influenced by the air
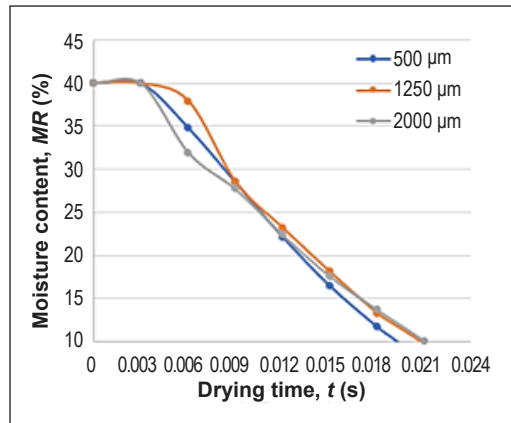

(a)
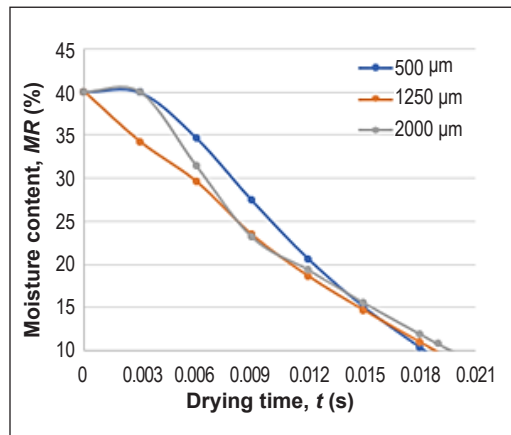
(b)
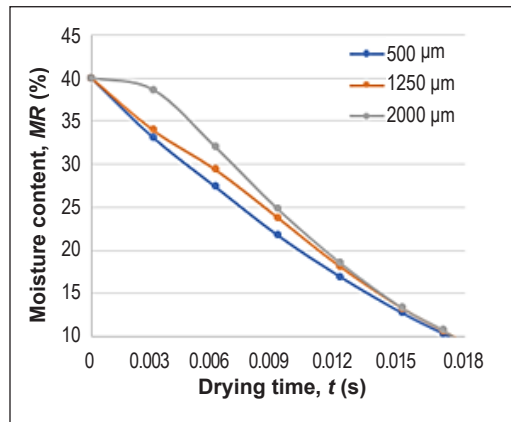
(c)

Figure 8. Moisture content against drying times at different diameters of sago at temperature: (a) 50°C; (b) 70°C; and (c) 90°C

temperature, and drying using FBD produces a uniform gas distribution (Okoronkwo et al., 2013; Silva et al., 2017). This results in the uniform drying of sago waste, which helps speed the drying process. The uniform drying in FBD and the air temperature are the primary factors significantly impacting the drying process. Consequently, the diameter of sago waste has a minimal effect on the drying process, particularly at high temperatures.

Analysis of Variance (ANOVA) and Estimated Regression of Each Response

Analysis of variance was performed to validate the accuracy of this FBD model and simulation result, where an average squared, degrees of freedom, sum squared, F-values, and P-values were used to check the model's effectiveness. The variance of the data about the mean was estimated by determining the F-value. In addition, the P-value validates the model from a statistical point of view. According to the variance analysis, the parameter has more accuracy at higher F-values than one. Furthermore, P values less than 0.05 mean that the model is approved from a statistical point of view. Based on the result in Table 4, the F-value for this FBD model is 98.41, indicating that the model is important. A P-value of less than 0.05 indicates that the model term is important. Next, A-temperature and B-Air velocity are important model terms. At the same time, the C-diameter of sago waste is an insignificant model term because the P-value shows a value greater than 0.1. The R^2 and adjusted-R^2 values for these FBD models are 0.9486 and 0.9390, respectively. The predicted R^2 is 0.9108, which shows a reasonable agreement. These values for sufficient accuracy are used to measure the signal-to-sound ratio. Sufficient accuracy compares the range of forecast values at the design point with the average forecast error, where ratios with values greater than 4 are desirable. The ratio of 31.9996 indicates an adequate signal-to-noise ratio. Thus, it can be concluded that this FBD model can be used to navigate the design space.

Based on Table 4, the F-value model of 2416.19 indicates that the model is important. The values for sufficient accuracy are used to measure the signal-to-sound ratio. The R^2 and

Table 4
Analysis of variance for moisture content

Source	Sum of Squares	df	Mean Square	F-value	p-value
Model	**279.19**	**3**	**93.06**	**98.41**	**< 0.0001**
A-Temperature	33.76	1	33.76	35.69	< 0.0001
B-Air velocity	245.15	1	245.15	259.23	< 0.0001
C-Sago bagasse diameter	0.2880	1	0.2880	0.3045	0.5887
Residual	15.13	16	0.9457		
Lack of Fit	15.13	11	1.38		
Pure Error	0.0000	5	0.0000		
Cor Total	294.32	19			
R^2	0.9486		Adeq Precision: 31.9996		

adjusted-R^2 values for the models are 0.9995 and 0.9991, respectively. The predicted R^2 of 0.9964 is in reasonable agreement. Sufficient accuracy is determined by comparing the range of forecast values at the design point with the average forecast error. Using a ratio value higher than 4 is desirable. The ratio of 138.97 indicates an adequate signal-to-noise ratio. So, this FBD model can be used to navigate the design space. It can be concluded that the analysis of variance for the quadratic model in Table 5 shows that the values for temperature (A), sago waste diameter (C), sago waste diameter temperature (AC), and square sago waste diameter (C2) have p-values less than 0.05, that suggests all four terms are important.

Table 5
Analysis of variance for moisture diffusivity (D_{eff})

Source	Sum of Squares	df	Mean Square	F-value	p-value
Model	5.57	9	0.6192	2416.19	< 0.0001
A-Temperature	0.0123	1	0.0123	47.88	< 0.0001
B-Air velocity	0.0002	1	0.0002	0.7304	0.4128
C-Sago bagasse diameter	5.55	1	5.55	21643.92	< 0.0001
AB	0.0001	1	0.0001	0.5128	0.4903
AC	0.0059	1	0.0059	23.19	0.0007
BC	0.0001	1	0.0001	0.2336	0.6393
A²	0.0018	1	0.0018	7.06	0.0240
B²	0.0001	1	0.0001	0.3111	0.5893
C²	0.0005	1	0.0005	1.78	0.2117
Residual	0.0026	10	0.0003		
Lack of Fit	0.0026	5	0.0005		
Pure Error	0.0000	5	0.0000		
Cor Total	5.58	19			
R²	0.9995			Adeq Precision:138.97	

Optimization Analysis

The results of optimizing sago waste drying in FBD are shown in Table 6. It shows the optimum values of temperature control factor, inlet air velocity, and sago waste diameter are at T=90°C, vi=2.1 m/s, and dp=2000 μm with the highest desirability value of 0.981. The predicted moisture content and Deff values of sago waste are 10.439% and 2.016 m²/s, respectively. The detailed comparison between the RSM predicted analysis and the CFD simulation result is listed in Table 7. Based on the table, the errors between this CFD simulation results and RSM predictions are 0.03% and 0.04% for sago waste moisture content and D_{eff} values, respectively, indicating that the predictions generated by the RSM model are accurate.

Figure 9 shows the overall desirability for the combination of inlet temperature and air velocity by the response surface plot for the optimized sago waste diameter dp=2000 μm.

Table 6
Results of optimization of the drying process in FBD

Temperature	Air velocity	Sago bagasse diameter	Moisture content	$D_{efft} \times 10^{-2}$	Desirability
90.000	2.100	2000.000	10.439	2.016	0.981
89.827	2.100	2000.000	10.455	2.016	0.980
90.000	2.100	1993.748	10.438	2.010	0.979
90.000	2.098	1999.999	10.480	2.016	0.979
89.533	2.100	1999.999	10.482	2.016	0.979
90.000	2.095	1999.999	10.529	2.016	0.977
90.000	2.100	1982.818	10.437	1.999	0.977
88.903	2.100	1999.998	10.540	2.016	0.977
90.000	2.100	1977.026	10.434	1.993	0.976
88.535	2.100	2000.000	10.574	2.015	0.975
90.000	2.091	2000.000	10.592	2.017	0.975
89.817	2.100	1970.962	10.450	1.987	0.974
88.067	2.100	1999.998	10.617	2.015	0.973
90.000	2.088	1998.705	10.636	2.015	0.972

Table 7
Comparison between the RSM predicted value and the CFD simulation result

	Temperature	Air velocity	Sago diameter	Moisture content	$D_{efft} \times 10^{-2}$
RSM prediction	90	2.1	2000	10.439	2.106
CFD simulation				10.72	2.014
Error(%)	-	-	-	0.03	0.04

This desirability surface plot shows that the control factor values A=90°C and B=2.1 m/s are required to obtain desirability values D=0.981. Moreover, the surface plot shows that the air velocity and the air temperature play a role in the optimization process with the obtained desirability value of 0.981. It indicates that the RSM model is accurate and close to the ideal value because the reliability value lies between 0 and 1, and it represents the proximity of the response to its ideal value. If the reaction is in an unacceptable interval, its desirability value is 0, and if the reaction is in the ideal interval or reaches its ideal value, its desirability is
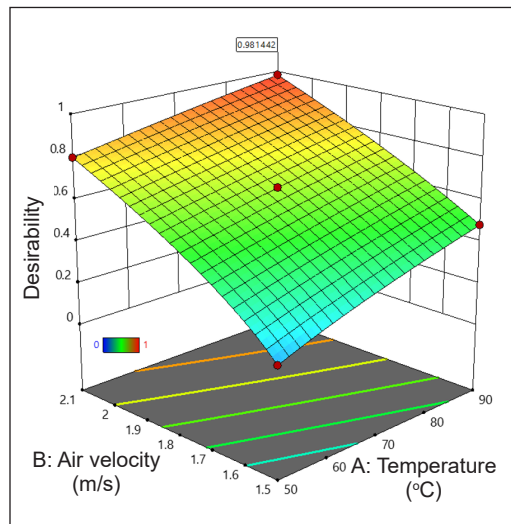

Figure 9. Desirability surface plot for sago bagasse diameter 2000 µm

1 (Rafik, 2016). Besides, a previous study obtained a tolerability value of D=0.781 with optimal conditions for the optimized reaction combination where the input temperature was at T=90°C, and the input velocity was v_i=5 m/s, and the square geometry for cut drying Apple (Majdi et al., 2019).

Validation of CFD Model and RSM Optimization Parameters with Experimental Data

Comparing the present study's findings with those of a previous study is essential to evaluate the progress and innovation achieved. In the case of drying efficiency, the present study applied the model-driven approach, which significantly improved drying efficiency, reducing the drying time required for sago bagasse. Besides, the systematic variation of parameters, including particle diameter, hot air temperature, and inlet air velocity, contributed to a more efficient moisture removal process. In the previous studies, it was challenging to provide a direct comparison in the absence of a wide range of drying parameters during the experimental process. However, this model-driven approach suggests potential improvements in drying efficiency over traditional methods. In the case of optimal conditions, this present study found that the optimal conditions for sago drying were obtained through the RSM. These conditions were tailored to maximize drying efficiency and product quality. Meanwhile, the details about optimal conditions in the previous study are unavailable for direct comparison. Thus, this present study compared the findings with the limitation of the experiment data conducted by Rosli et al. (2020), where the FBD model developed using CFD and optimized by the RSM approach was validated at v_i =2.1 m/s and d_p=2000 μm as shown in Figure 10. Figure 10(a) shows the results of experiments conducted by Rosli et al. (2020), and Figure 10(b) shows the CFD result obtained from this present study. Both results show a similar trend where the moisture content of sago waste decreases with a longer drying time but increases with a higher temperature.


<table>
<tr><td>(a)</td><td>(b)</td></tr>
</table>
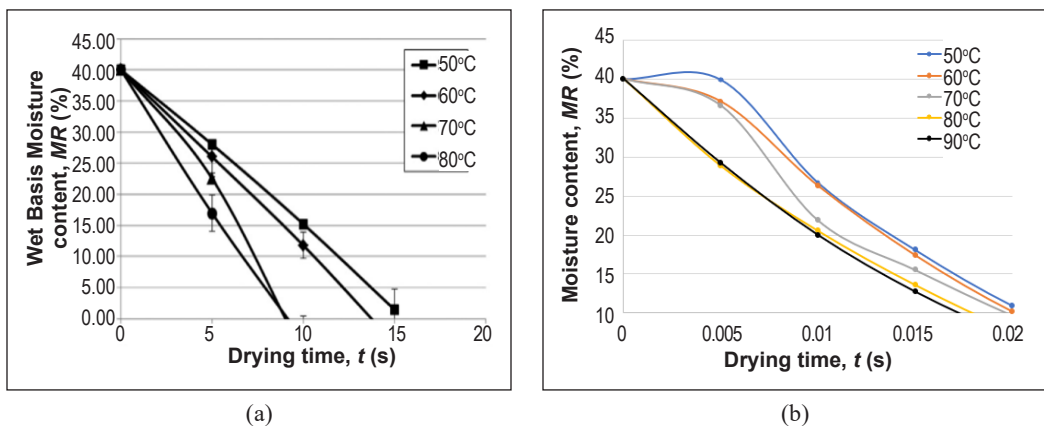
Figure 10. Moisture content against drying time of: (a) Previous studies; and (b) this CFD simulation

In addition, the current study hints at sustainability improvements through reduced energy consumption, which indirectly impacts environmental sustainability and the reduction of greenhouse gas emissions. However, the sustainability aspects in the previous study were not discussed. In summary, while the present study demonstrates the potential for significant advancements in sago drying efficiency and product quality through a model-driven approach, specific comparative data or findings from a previous study were not available for a direct, detailed comparison. However, the present study lays the groundwork for potential improvements and innovations in sago drying, which may have far-reaching implications for sago production, consumption, and the broader food industry. Future research could further build upon these findings and investigate the real-world implementation of the model-driven approach.

CONCLUSION

A two-dimensional model of an FBD for drying sago waste has been successfully constructed using ANSYS® DesignModelerTM 2020 R2 software. The mesh dependence test was carried out after the construction of the geometry, and the mesh size used was 1.5 mm. The simulations were performed until the moisture content was reduced to 10%. The CFD model was validated by comparing it with previous studies by Rosli et al. (2020). The analysis of the moisture content of sago waste was carried out at different inlet air velocities, inlet air temperatures, and diameters of sago waste at v_i=1.5-2.1 m/s with a diameter of d_p=500-2000 μm and T=50-90°C. The simulation results showed that a drying temperature of T=90°C dried the sago waste faster than other temperatures. Sago waste was dried quickly at v_i=2.10 m/s as the hot air entering the drying chamber was at a higher air velocity. This condition increased the diffusion of hot air in the dryer, increasing the amount of water that can evaporate. In addition, the diameter of sago waste affects its moisture content at lower drying temperatures because uniform drying in FBD and air temperature factors significantly influence the drying process. Consequently, the diameter of sago waste has minimal effect on the drying process at high temperatures. Besides the RSM method, the Design Expert® 7.00 (DX7) software was used to optimize the sago waste drying process. It showed that the optimum drying process occurred at T=90°C, v_i=2.1 m/s, and d_p=2000 μm. Since the obtained desirability value is 0.981, the RSM model is accurate and close to the ideal value.

ACKNOWLEDGEMENT

REFERENCES

Antony, J., & Shyamkumar, M. B. (2016). Study on sand particles drying in a fluidized bed dryer using CFD. *International Journal of Engineering Studies, 8*(2), 129-145.

Arumuganathan, T., Manikantan, M. R., Ramanathan, M., Rai, R. D., Indurani, C., & Karthiayani, A. (2017). Effect of diffusion channel storage on some physical properties of button mushroom (Agaricus *bisporus*) and shelf-life extension. *Proceedings of the National Academy of Sciences, India Section B: Biological Sciences*, 87(3), 705-718. https://doi.org/10.1007/s40011-015-0628-4

Assawarachan, R. (2013). Drying kinetics of coconut residue in fluidized bed. *International Journal of Agriculture Innovations and Research, 2*(2), 263–266.

Azmir, J., Hou, Q., & Yu, A. (2018). Discrete particle simulation of food graindrying in a fluidised bed. *Powder Technology*, *323,* 238-249. https://doi.org/10.1016/j.powtec.2017.10.019

Dechsiri, C. (2004). *Particle Transport in Fluidized Beds: Experiments and Stochastic Models.* [Unpublished Doctoral thesis]. University of Groningen.

Gazor, H. R., & Mohsenimanesh, A. (2010). Modelling the drying kinetics of canola in fluidised bed dryer. *Czech Journal of Food Sciences*, *28*(6), 531-537. https://doi.org/10.17221/256/2009-CJFS

Halim, L. A., Basrawi, M. F., Faizal, S. N., Yudin, A. S. M., & Yusof, T. M. (2020). Effect of superficial air velocity on the fluidized bed drying performance of stingless bee pot-pollen. *IOP Conference Series: Materials Science and Engineering, 863*(1), Article 012041. https://doi.org/10.1088/1757-899X/863/1/012041

Han, M. (2015). *Characterization of Fine Particle Fluidization*. [Doctoral dissertation]. The University of Western Ontario. https://ir.lib.uwo.ca/etd/3073

Hasibuan, R., Pane, Y. M., & Hanief, S. (2018, August 30-31). *Effect of air velocity and thickness to drying rate and qualitytemulawak (Curcum xanthorrhiza roxb) using combination solar moleculer sieve.* [Paper presentation]. The International Conference of Science, Technology, Engineering, Environmental and Ramification Researches-ICOSTEERR, Sumatera Utara, Indonesia. https://doi.org/10.5220/0010103503890394

Li-Zhen, D., Arun, S.M., Qian, Z., Xu-Hai, Y., Jun, W., Zhi-An, Z., Zhen-Jiang, G., & Hong- Wei, X. (2019). Chemical and physical pretreatments of fruits and vegetables: Effects on drying characteristics and quality attributes – A comprehensive review. *Critical Reviews in Food Science and Nutrition,* 59(9), 1408-1432. https://doi.org/10.1080/10408398.2017.1409192

Luthra, K., & Sadaka, S. S. (2020). Challenges and opportunities associated with drying rough rice in fluidized bed dryers: A review. *American Society of Agricultural and Biological Engineers, 63*(3), 583-595. https://doi.org/10.13031/trans.13760

Maheswari, S. U. (2015). Drying of pearl millet using fluidised bed dryer: Experiments and modelling. *International Journal of ChemTech Research*, *8*(1), 377-387.

Majdi, H., Esfahani, J. A., & Mohebbi, M. (2019). Optimization of convective drying by response surface methodology. *Computers and Electronics in Agriculture*, *156*, 574-584. https://doi.org/10.1016/j.compag.2018.12.021

Malekjani, N., & Jafari, S. M. (2018). Simulation of food drying processes by computational fluid dynamics (CFD): Recent advances and approaches. *Trends in Food Science & Technology*, *78*, 206-223. https://doi.org/10.1016/j.tifs.2018.06.006

Mortier, S. T. F., De Beer, T., Gernaey, K. V., Remon, J. P., Vervaet, C., & Nopens, I. (2011). Mechanistic modelling of fluidized bed drying processes of wet porous granules: A review. *European Journal of Pharmaceutics and Biopharmaceutics*, *79*(2), 205-225. https://doi.org/10.1016/j.ejpb.2011.05.013

Naim, H. M., Yaakub, A. N., & Hamdan, D. A. A. (2016). Commercialization of sago through estate plantation scheme in Sarawak: The way forward. *International Journal of Agronomy*, *2016*, Article 8319542. https://doi.org/10.1155/2016/8319542

Nasir, A. M. A., Rosli, M. I., Takriff, M. S., Othman, N. T. A., & Ravichandar, V. (2021). Computational fluid dynamics simulation of fluidized bed dryer for sago pith waste drying process. *Jurnal Kejuruteraan*, *33*(2), 239-248. https://doi.org/10.17576/jkukm- 2021-33(2)-09

Norhaida, H. A. T., Ang, W. L., Kismurtono, M., & Siti, M. T. (2020). Effect of air temperature and velocity on the drying characteristics and product quality of *Clinacanthus* nutans in heat pump dryer. *IOP Conference Series: Earth and Environmental Science, 462*(1), Article 012052. https://doi.org/10.1088/1755-1315/462/1/012052

Okoronkwo, C. A., Nwufo, O. C., Nwaigwe, K. N., Ogueke, N. V., & Anyanwu, E. E. (2013). Experimental evaluation of a fluidized bed dryer performance. *The International Journal of Engineering and Science, 2*(6), 45-53.

Othman, N. T. A., & Ivan, A. H. (2021). Development of a fluidized bed dryer for drying of a sago bagasse. *Pertanika Journal of Science & Technology, 29*(3), 1831-1845 https://doi.org/10.47836/pjst.29.3.13

Pusat, S., Akkoyunlu, M. T., Erdem, H. H., & Teke, I. (2015). Effects of bed height and particle size on drying of a Turkish lignite. *International Journal of Coal Preparation and Utilization*, *35*(4), Article 150203135736008. https://doi.org/10.1080/19392699.2015.1009051

Puspasari, I., Meor, Z., Wan Daud, D., & Tasirin, S. (2014). Characteristic drying curve of oil palm fibers. *International Journal on Advanced Science, Engineering and Information Technology, 4*(1), 20-24. https://doi.org/10.18517/ijaseit.4.1.361

Rashid, M. R. M., Johari, M. A. M., & Ahmad, Z. A. (2016). Sago pith waste ash as a new alternative raw materials from agricultural waste. *Materials Science Forum*, *840,* 389-393. https://doi.org/10.4028/www.scientific.net/MSF.840.389

Rosli, M. I., Abdul Nasir, A. M., Takriff, M. S., & Lee, P. C. (2018). Simulation of a fluidized bed dryer for the drying of sago waste. *Energies*, *11*(9), Article 2383. https://doi.org/ 10.3390/en11092383

Rosli, M. I., Nasir, A. A., Takriff, M. S., & Ravichandar, V. (2020). Drying sago pith waste in a fluidized bed dryer. *Food and Bioproducts Processing*, *123*, 335-344. https://doi.org/10.1016/j.fbp.2020.07.005

Sarker, M. S. H., Ibrahim, M. N., Aziz, N. A., & Punan, M. S. (2015). Energy and exergy analysis of industrial fluidized bed drying of paddy. *Energy, 84*, 131-138. https://doi.org/10.1016/j.energy.2015.02.064

Shukrie, A., Anuar, S., & Oumer, A. N. (2016). Air distributor designs for fluidized bed combustors: A review. *Engineering, Technology & Applied Science Research*, *6*(3), 1029-1034. https://doi.org/10.48084/etasr.688

Silva, B. G., Fileti, A. M. F., Foglio, M. A., Rosa, P. D. T. V., & Taranto, O. P. (2017). Effects of different drying conditions on key quality parameters of pink peppercorns (Schinus terebinthifolius Raddi). *Journal of Food Quality*, *2017*, Article 3152797. https://doi.org/10.1155/2017/3152797

Tamboli, T. G., & Bhong, M. G. (2018). Review on different drying methods: Applications & advancements. *International Journal on Theoretical and Applied Research in Mechanical Engineering*, *7*(1), 33-40.

Wang, A. H., & Chen, G. (2000). Heat and mass transfer in batch fluidized-bed drying of porous particles. *Chemical Engineering Science, 55*(10), 1857-1869. https://doi.org/10.1016/S0009-2509(99)00446-7

Wee, O. Y., Ling, L. P., Bujang, K., & Fong, L. S. (2017). Physiochemical characteristic of sago (*Metroxylon sagu)* starch production wastewater effluents. *International Journal of Research in Advent Technology, 5*(9), 4-13.

Zhang, W., Cheng, X., Hu, Y., & Yan, Y. (2017). Measurement of moisture content in a fluidized bed dryer using an electrostatic sensor array. *Powder Technology, 325*, 49-57. https://doi.org/10.1016/j.powtec.2017.11.006